

# Chapter 3

## Magnetic Domains

### 3.1 Ferromagnetism and domain theory

#### 3.1.1 Atomic origin of ferromagnetism

Bulk magnetic behaviour arises from the magnetic moments of individual atoms. There are two contributions to the atomic magnetic moment from the momentum of electrons. Firstly, each electron has an intrinsic magnetic moment and an intrinsic angular momentum (spin). Secondly, electrons may also have a magnetic moment and an angular momentum as a result of their orbital motion in atoms.

The Pauli exclusion principle permits only one electron in an atom to have a particular combination of the four quantum numbers  $n$ ,  $l$ ,  $m_l$  and  $m_s$ . The first three numbers specify the electron energy state. The spin quantum number,  $m_s$ , can only take the values  $\pm 1/2$ . Each energy state may therefore contain up to two electrons. If only one electron is present, its spin moment contributes to the overall spin moment of the atom. A second electron is required to have an antiparallel spin to the first, and the two spins will cancel out, giving no net moment. Strong magnetic properties are associated with elements which have a large number of unpaired spins.

In solid materials, the orbital moments are strongly coupled to the crystal lattice and are therefore unable to change direction when a magnetic field is applied. Because of this ‘orbital quenching’, the magnetic moments in solids can be considered as due to the spins only. An atom with uncompensated

spins has a net magnetic moment in the absence of an applied field; solids composed of such atoms are termed ‘paramagnetic’. In general, the atomic magnetic moments in paramagnets are randomly aligned when no field is present, and the magnetisation process consists of aligning them into the field direction. However, some paramagnetic materials undergo a transition on cooling to an ordered state in which there is local alignment of atomic moments. The ordered state is ‘ferromagnetic’ if adjacent atomic moments are aligned parallel to one another, and ‘ferrimagnetic’ if they are antiparallel but of different magnitude such that there is a local net magnetisation.

The temperature of the order/disorder transition is known as the Curie temperature ( $T_C$ ) in ferromagnets. The degree of ordering increases with decreasing temperature. Iron in its body-centred cubic (b.c.c.) ferrite form is strongly ferromagnetic, as are many widely used steels. In the ferritic power plant steels discussed in Chapter 2, the austenitisation treatment takes the steel above its Curie temperature, and it becomes paramagnetic. Air-cooling or quenching to give bainite or martensite gives a b.c.c. or body-centred tetragonal structure which is ferromagnetic, and the ferromagnetism is retained on tempering.

### 3.1.2 Weiss domain theory

Weiss (1906, 1907) postulated that atoms in ferromagnetic materials had permanent magnetic moments which were aligned parallel to one another over extensive regions of a sample. This was later refined into a theory of ‘domains’ of parallel moments (Weiss, 1926). The overall magnetisation (magnetic moment per unit volume) of a block of material is the vector sum of the domain magnetisations. In the demagnetised state, this is zero. As a field is applied, changes in the domain configuration, for example in the relative widths of domains, allow a net magnetisation in the field direction. Weiss’ hypothesis was later confirmed by direct observation (Bitter, 1931), and the concept of magnetostatic energy, which explained the formation of domains, was proposed by Landau and Lifshitz (1935).

### 3.1.3 Ideal domain structure

In a homogeneous, defect-free, single-crystal ferromagnet with cubic symmetry, the domain structure can be explained by a balance between four energy terms: exchange, magnetostatic, anisotropy and magnetoelastic (Kittel and Galt, 1956).

#### Exchange energy

Weiss extended an existing statistical thermodynamic theory for paramagnetism (Langevin, 1905), to describe the alignment of the atomic magnetic moments within domains. The Weiss ‘mean field’  $\mathbf{H}_e$  in the original theory was given by:

$$\mathbf{H}_e = \alpha \mathbf{M} \quad (3.1)$$

where  $\mathbf{M}$  is the magnetisation, and  $\alpha$  is the ‘mean field constant’. The mean field approximation requires that all magnetic moments interact equally with all others. Although this is obviously a simplification of the true situation, it is nevertheless a useful concept for consideration of the atoms within domains, which usually extend over  $10^{12}$  to  $10^{18}$  atoms. The origin of the interaction was later identified by Heisenberg (1928) as a quantum-mechanical exchange effect due to overlapping wavefunctions of neighbouring atoms. If only nearest neighbours are considered, the exchange energy  $E_{ex}$  per unit volume associated with this interaction is:

$$E_{ex} = -2\beta \sum_i \sum_j \mathbf{m}_i \cdot \mathbf{m}_j \quad (3.2)$$

where  $\beta$  is a term characterising the strength of the interaction, and the summation is over all nearest-neighbour pairs  $i$  and  $j$  in a unit of volume. In ferromagnetic materials,  $\beta$  is positive, giving a minimum exchange energy when moments lie parallel. Complete alignment of all atomic moments in the sample (magnetic saturation) is therefore favoured by this term. An explanation is therefore needed of how the demagnetised state can arise; this is given by the magnetostatic energy term.

### Magnetostatic energy

A body of magnetisation  $\mathbf{M}$  in a magnetic field  $\mathbf{H}$  has a magnetostatic energy  $E_m$  arising from the interaction of  $\mathbf{M}$  with  $\mathbf{H}$ :

$$E_m = -\mu_0 \int \mathbf{H} \cdot \partial\mathbf{M} \quad (3.3)$$

where  $\mu_0$  is the permeability of free space. At any internal or external surface of a uniformly magnetised body, there is a discontinuous change in the component of  $\mathbf{M}$  normal to the surface, which can be envisaged as a source of ‘free poles’. These are magnetic (north or south) poles which are not compensated by poles of the opposite kind in the immediate vicinity. They produce a demagnetising field, which favours a change in the arrangement of magnetic moments such that the poles disappear. A finite body has free poles on its outer surfaces, resulting in a demagnetising field  $\mathbf{H}_d$  antiparallel to the magnetisation  $\mathbf{M}$ ; this tends to turn  $\mathbf{M}$  so that it points parallel to the surfaces. This field is given by:

$$\mathbf{H}_d = N_d \mathbf{M} \quad (3.4)$$

where  $N_d$  is the demagnetising factor, which depends only on sample geometry. For a sample with magnetisation  $\mathbf{M}$  but no applied field, the magnetostatic energy depends only on  $\mathbf{M}$  and  $N_d$ , and can be obtained by substituting Equation 3.4 into Equation 3.3 to give:

$$E_d = \frac{\mu_0}{2} N_d M^2 \quad (3.5)$$

In the absence of an applied field, the magnetostatic energy is therefore a minimum when the magnetisation is zero, and subdivision into domains is favoured (Figure 3.1 (a), (b)). Reducing the domain width decreases the spatial extent of the field and hence the energy (c). If domains magnetised at  $90^\circ$  to the main domains can form, external free poles can be eliminated entirely, reducing the magnetostatic energy to zero (Figure 3.1 (d)).

Demagnetising factors can be determined exactly for ellipsoids of revolution only, but approximate values have been calculated for commonly used sample shapes, such as cylinders (Chen *et al.*, 1991).

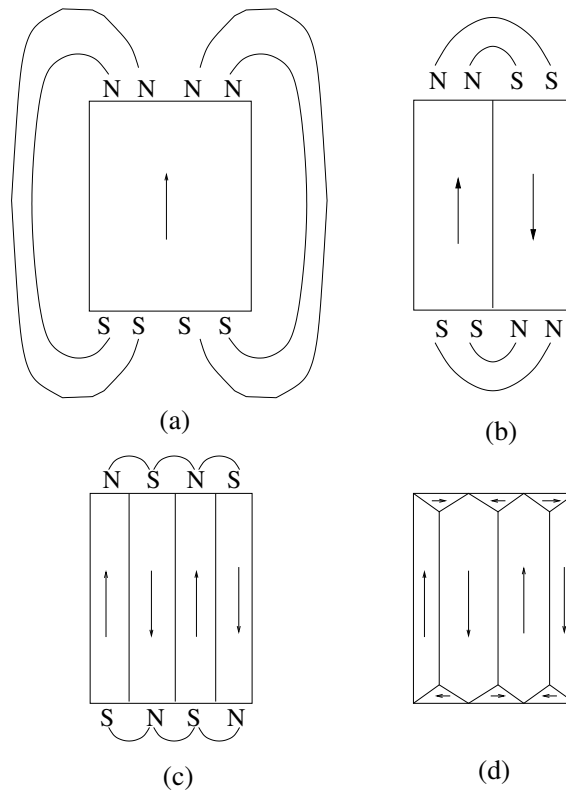


Figure 3.1: Subdivision into domains (cubic material with positive anisotropy). (a) a saturated sample, with high demagnetising energy  $E_d$ ; (b) splitting into two reduces  $E_d$ ; (c) more splitting reduces  $E_d$  further; (d) free poles eliminated by closure domains. After Kittel and Galt, 1956.

### Crystalline anisotropy energy

Magnetocrystalline anisotropy is the preferential alignment of atomic magnetic moments along certain, ‘easy’ crystal directions. Other, ‘hard’ directions are particularly unfavourable. This arises from coupling between the spin and orbital moments (Brooks, 1940). The orbital moments are constrained in their directions by the crystal lattice, so the crystal symmetry influences the behaviour of the spins through this coupling.

To a first approximation, the anisotropy energy  $E_a$  per unit volume for a material with cubic symmetry is given by:

$$E_a = K_1(\alpha_1^2\alpha_2^2 + \alpha_2^2\alpha_3^2 + \alpha_3^2\alpha_1^2) \quad (3.6)$$

where  $K_1$  is a constant of proportionality known as the anisotropy constant, and  $\alpha_1$ ,  $\alpha_2$  and  $\alpha_3$  are the cosines of the angles made by magnetisation vector with the crystal axes  $x$ ,  $y$  and  $z$ . In b.c.c. iron,  $K_1$  is positive, and the cube edges  $\langle 100 \rangle$  are the easy directions (Honda and Kaya, 1926). Antiparallel magnetisation directions are crystallographically equivalent, giving three distinct easy directions for positive- $K_1$  materials. This allows the formation of closure domains oriented at  $90^\circ$  to the main domains (Figure 3.1 (d)).

### Magnetoelastic energy

If a cubic single crystal is magnetised to saturation in a direction defined by the direction cosines  $\alpha_1$ ,  $\alpha_2$  and  $\alpha_3$  with respect to the crystal axes  $x$ ,  $y$  and  $z$ , a magnetostrictive strain  $\lambda_{si}$  is induced in a direction defined by the cosines  $\beta_1$ ,  $\beta_2$  and  $\beta_3$ :

$$\lambda_{si} = \lambda_{100} \left( \alpha_1^2\beta_1^2\alpha_2^2\beta_2^2\alpha_3^2\beta_3^2 - \frac{1}{3} \right) + 3\lambda_{111}(\alpha_1\alpha_2\beta_1\beta_2 + \alpha_2\alpha_3\beta_2\beta_3 + \alpha_3\alpha_1\beta_3\beta_1) \quad (3.7)$$

where  $\lambda_{100}$  and  $\lambda_{111}$  are the magnetostriction constants along  $\langle 100 \rangle$  and  $\langle 111 \rangle$  respectively.  $\lambda_{si}$  is the ‘ideal’ magnetic field-induced magnetostriction. This is defined by Cullity (1971) as the strain induced when a specimen is brought to technical saturation (§ 3.2.1) from the ideal demagnetised state, *i.e.* the state in which all of the domain orientations allowed by symmetry are present in equal volumes.

If magnetostriction is isotropic, *i.e.*  $\lambda_{100} = \lambda_{111} = \lambda_{si}$ , then Equation 3.7 may be simplified to:

$$\lambda_\theta = \frac{3}{2}\lambda_{si} \left( \cos^2 \theta - \frac{1}{3} \right) \quad (3.8)$$

where  $\lambda$  is the magnetostriction measured at an angle  $\theta$  to the magnetisation and the field.

In practice, however, the magnetostriction is not ideal, but depends on the magnetic history of the material and the thermomechanical treatment

to which it has been subjected. It is possible, for example, to produce a preferred orientation of magnetic domains by annealing in a magnetic field (*e.g.* review by Watanabe *et al.*, 2000).

If a domain is constrained by its neighbours, magnetostriction manifests itself as a strain energy rather than a dimensional change. Maintaining coherence between the closure domains and the main domains in Figure 3.1 (d) requires a strain energy proportional to the volume of the closure domains. This can be reduced, while maintaining the closure effect, by increasing the number both of closure domains and main domains. However, this requires more domain walls to be created; since, as will be discussed below, domain walls have a higher energy than the bulk, the equilibrium configuration is determined by a balance between domain wall and magnetoelastic energy contributions.

In polycrystals with no preferred orientation, the magnetostriction constant  $\lambda_{si}$  will be an average of the values of all the crystal orientations. To obtain an estimate for this average, assumptions must be made about the grain size and the transfer of stress or strain between grains. The expressions obtained depend on these assumptions unless the grains are elastically isotropic (Cullity, 1971).

### 3.1.4 Energy and width of domain walls

The transition region between domains magnetised in different directions was first studied by Bloch (1932). The change from one direction to the other is not discontinuous but occurs over a width determined by a balance between exchange and anisotropy energy. The energy and thickness of various types of domain walls have been calculated (Kittel and Galt, 1956).

The mean field approximation breaks down at domain walls, but the exchange energy per moment,  $E_{ex}$ , can be calculated by considering only nearest-neighbour interactions and neglecting others. For neighbouring moments  $\mathbf{m}_i$  and  $\mathbf{m}_j$ ,  $E_{ex}$  is given by:

$$E_{ex} = -\mu_0 z \mathcal{J} \mathbf{m}_i \cdot \mathbf{m}_j \quad (3.9)$$

where  $\mathcal{J}$  is a term characterising nearest-neighbour interactions and  $z$  is the number of nearest neighbours<sup>1</sup>. If the angle between  $\mathbf{m}_i$  and  $\mathbf{m}_j$  is  $\phi$ ,

$$E_{ex} = -\mu_0 z \mathcal{J} m^2 \cos \phi \quad (3.10)$$

For a linear chain of moments, each has two nearest neighbours. Substituting the small-angle approximation  $\cos \phi = 1 - \phi^2/2$  gives:

$$E_{ex} = \mu_0 \mathcal{J} m^2 (\phi^2 - 2) \quad (3.11)$$

A wall separating domains magnetised at  $180^\circ$  to one another, and extending across  $n$  lattice parameters of size  $a$ , has an exchange energy per unit area  $\frac{E_{ex}}{a^2}$ :

$$\frac{E_{ex}}{a^2} = \frac{\mu_0 \mathcal{J} m^2 \phi^2 \pi^2}{n a^2} \quad (3.12)$$

$E_{ex}$  is therefore lowest when  $n$  is large, favouring wide walls.

The anisotropy energy of the  $p$ th moment in a wall can be approximated as:

$$E_a = (K_1/4) \sin^2 2p\phi \quad (3.13)$$

where  $K_1$  is the anisotropy constant. Summing this over the domain wall width gives an anisotropy energy per unit area:

$$E_a = K_1 n a \quad (3.14)$$

where  $a$  is the lattice spacing and  $n$  the number of layers of atoms in the domain wall.  $E_a$  increases with  $n$ , favouring a narrow wall. The total wall energy per unit area  $\gamma = E_{ex} + E_a$  is minimised by differentiating with respect to the wall width  $\delta = n a$  and setting the derivative to zero.

$$\frac{\partial \gamma}{\partial \delta} = \frac{-\mu_0 \mathcal{J} m^2 \pi^2}{\delta^2 a} + K_1 = 0 \quad (3.15)$$

Hence,

---

<sup>1</sup>This is of a similar form to Equation 3.2 but in this case is expressed per moment.

$$\delta = \sqrt{\frac{\mu_0 \mathcal{J} m^2 \pi^2}{K_1 a}} \quad (3.16)$$

Using these expressions, Jiles (1998) has estimated the width of a wall separating antiparallel domains in iron as 40 nm, or 138 lattice parameters, and its energy as  $3 \times 10^{-3} \text{ J m}^{-2}$ .

### 3.1.5 Determination of the equilibrium domain structure

To obtain the minimum-energy configuration of an assembly of domains so that the equilibrium structure can be found, a set of differential equations must be solved. These micromagnetics equations (Brown, 1963) assume continuously varying atomic moments, and are therefore difficult to solve for large-scale arrays of domains. In practice, a less complex ‘domain theory’ is applied, which treats each domain as uniformly magnetised to saturation, with variations in direction occurring only within domain walls (Hubert and Schäfer, 2000). It is assumed throughout the rest of this discussion that, far from domain walls, the domain magnetisation is  $M_S$ , which is known as ‘saturation’ or ‘spontaneous’ magnetisation.

## 3.2 Evolution of domain structure on application of a magnetic field

### 3.2.1 Ideal magnetisation and demagnetisation

When a magnetic field  $\mathbf{H}$  is applied to a sample with no net magnetic moment, the energy balance previously existing is upset by the additional magnetostatic energy due to the field. The domain structure rearranges itself in order to minimise the energy under the new conditions.

In simple terms, at low  $H$  this occurs by the enlargement of domains with  $\mathbf{M}_S$  oriented approximately parallel to  $\mathbf{H}$  at the expense of those oriented antiparallel (Kittel and Galt, 1956). As  $H$  increases, domain walls are swept out. Rotations of domain magnetisation vectors into easy directions near

that of  $\mathbf{H}$  may also occur at intermediate fields. The resulting single domain has  $\mathbf{M}_S$  parallel to the easy direction nearest the direction of  $\mathbf{H}$ . At high field,  $\mathbf{M}_S$  is rotated against the anisotropy to lie exactly parallel to  $\mathbf{H}$ . This state is known as technical saturation. Further increases in the field give small increases in the magnetisation. Atomic moments deviate slightly from the applied field direction due to thermal activation, but higher applied fields reduce this deviation.

On reducing  $H$ , the domain magnetisation rotates into an easy direction, and the single domain subdivides by the nucleation of domains magnetised in the opposite direction to  $\mathbf{M}$  ('reverse domains').

The balance between the energy terms varies from one material to another, and this influences the exact details of magnetisation and demagnetisation. Ferritic iron has a high anisotropy constant  $K_1$ , so rotation out of the easy directions is difficult, and all low-field magnetisation changes can be attributed to domain wall motion (Shilling and Houze, 1974).

### 3.2.2 Magnetic hysteresis

In real materials, the magnetisation behaviour is influenced by microstructural defects and inhomogeneities, such as grain boundaries, dislocations, solutes, precipitates, inclusions, voids and cracks. Cycling between negative and positive applied field directions gives a hysteresis loop, in which  $\mathbf{M}$  takes different values depending on whether  $\mathbf{H}$  is increasing or decreasing. Magnetic hysteresis, which was first noted in iron by Warburg (1881) and described and named by Ewing (1900), results from energy losses incurred in magnetisation and demagnetisation. These are due in part to energetic interactions between domain walls and defects, and in part to rotation against the anisotropy.

### 3.3 Theories of domain wall-defect interactions

#### 3.3.1 Inclusions

##### Kersten inclusion theory

Since a domain wall has an energy per unit area (§ 3.1.4), this acts as a ‘surface tension’. An inclusion, such as a void or second-phase particle, embedded in the wall, reduces the wall energy in proportion to the area embedded (Kersten, 1943). For a spherical inclusion, the energy is minimised when the wall bisects the inclusion; this gives an energy reduction:

$$E_{area} = \pi r^2 \gamma \quad (3.17)$$

where  $r$  is the inclusion radius, and  $\gamma$  the wall energy per unit area (Figure 3.2). For rod- or plate-shaped inclusions, the energy reduction is greatest when the plane of largest area is parallel to the wall.

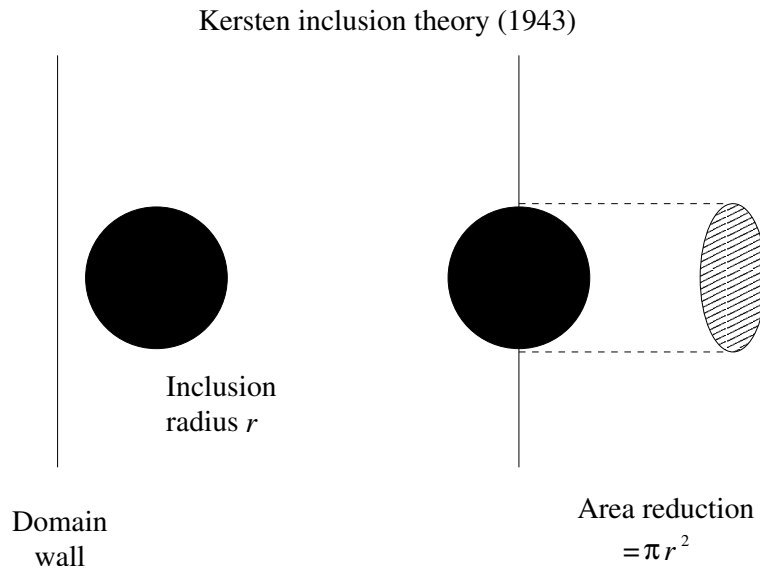


Figure 3.2: Energy reduction by intersection of inclusion with domain wall (Kersten, 1943).

### Néel inclusion theory

Néel (1944) demonstrated that energetic interactions between domain walls and inclusions also arise from internal demagnetising fields. In general, an inclusion has different magnetic properties from the bulk. If the normal component of magnetisation is discontinuous across the inclusion/matrix interface, a distribution of free poles will be present, giving a demagnetising field (Figure 3.3 (a)).

For a spherical, nonmagnetic inclusion of radius  $r$ , the associated magnetostatic energy is:

$$E_{demag} = \frac{8\pi^2 M_S^2 r^3}{9} \quad (3.18)$$

where  $M_S$  is the saturation magnetisation of the matrix. Positioning the domain wall so that it bisects the inclusion redistributes the free poles, approximately halving the demagnetising energy (Figure 3.3 (b)). It is not necessary that inclusions be nonmagnetic to cause demagnetising effects; for example,  $\text{Fe}_3\text{C}$  is ferromagnetic at room temperature, but has a pronounced effect on the magnetic properties of ferritic iron (Dykstra, 1969). It still behaves as a magnetic inhomogeneity in ferritic steel because its magnetic properties are different from those of the bulk (Jiles, 1998).

The Néel demagnetising effect scales with  $r^3$  (Equation 3.18), and therefore increases more rapidly than the Kersten area-reduction effect (Equation 3.17). However, for sufficiently large inclusions, it is energetically favourable to reduce the demagnetising energy of the inclusion by forming subsidiary domains around it, despite the additional domain wall energy involved. These thin, triangular ‘spike’ domains were predicted theoretically by Néel (1944) and subsequently observed by Williams (1947).

If an inclusion is bisected by a domain wall, closure domains can form, reducing the magnetostatic energy to zero (Cullity, 1972; Figure 3.4 (a)). When the main domain wall moves away from the inclusion under the action of an applied field, the subsidiary domain structure is drawn with it (Figure 3.4 (b)) before becoming irreversibly detached and forming spike domains (c).

Craik and Tebble (1965) calculated that inclusions whose diameter was

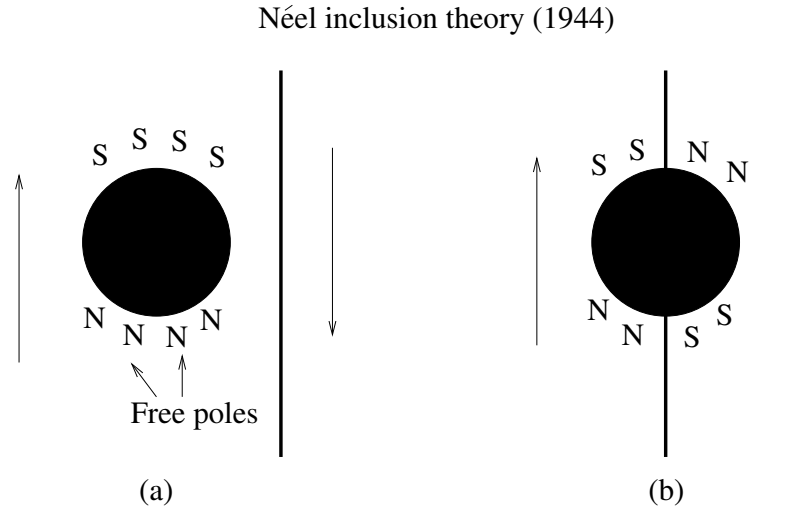


Figure 3.3: Distribution of free north (N) and south (S) poles around an inclusion (a) in the bulk (b) bisected by a domain wall (Néel, 1944).

equal to the domain wall width should be the most effective obstacles to domain wall motion.

For plate-like inclusions with magnetisation  $M_p$  having a planar interface with a matrix of magnetisation  $M_S$ , the free pole density at the interface  $\omega_{l^*}$  is given by:

$$\omega_{l^*} = \mu_0(M_S \cos \alpha_s - M_p \cos \alpha_p) \quad (3.19)$$

where  $\alpha_s$  and  $\alpha_p$  are the angles made by the magnetisations  $M_S$  and  $M_p$  with the interface (Goodenough, 1954). Goodenough proposed that the angle  $\alpha_p$  would adjust to minimise the total energy from free poles and the anisotropy of the inclusion.

### 3.3.2 Stress inhomogeneities

Stress affects the magnetic properties of a material via the converse of the magnetoelastic effect discussed above. The stress fields associated with vacancies, solute atoms and dislocations extend over a few atomic planes, but dislocations also interact with one another when sufficiently numerous, forming networks and tangles and creating a complex distribution of microstresses.

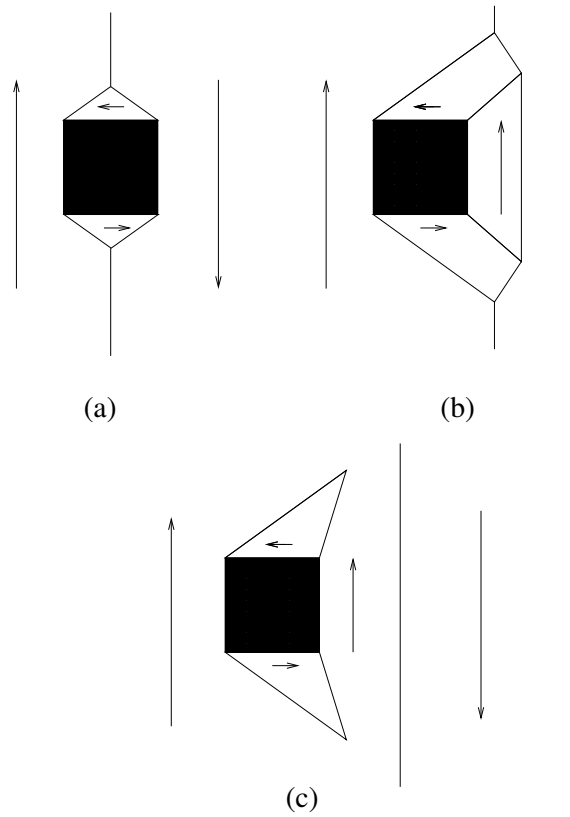


Figure 3.4: Interactions between domain wall and cubic inclusion with spikes (after Craik and Tebble, 1965): (a) domain wall at local energy minimum, (b) movement of main domain wall, (c) detachment of wall from inclusion.

The interaction between a domain wall and a stress field depends on the wall type (Träuble, 1969). ‘Type-II’ or ‘180°’ walls are those separating domains whose magnetisation directions are antiparallel to each other. In this case, since the magnetostrictive strain is independent of the sense of the magnetisation, there is no strain difference between the domains. For other angles, domain wall motion will modify the local strain energy. Domain walls of this kind are known as ‘Type-I’ or ‘non-180°’ walls.<sup>2</sup>

It is therefore likely that Type-I walls interact more strongly with stress fields than do Type-II walls. The local stress state would determine both

<sup>2</sup>They are also sometimes called ‘90°’ walls even in materials where the angle between the domains is not 90° .

the position and the energy of a Type-I wall, but the position of a Type-II wall would remain unchanged (Cullity, 1972). The longer-range interactions of Type-I walls with stress fields should make them less mobile, requiring a higher applied field before they will move (Träuble, 1969). As a result, magnetisation change at low applied fields is expected to occur predominantly by Type-II wall motion.

Calculations of the interaction force between domain walls and dislocations were made for several ideal cases by Träuble (1969). Scherpereel *et al.* (1970) calculated the energy of interaction of many different types of dislocations with Type-II and Type-I walls. On average, this was found to be higher for Type-II walls than for Type-I walls in iron, while the reverse was observed for nickel. This finding does not agree well with the model of Träuble. However, an experimental observation on an iron-based alloy appeared to support the Träuble interpretation (§ 3.4.2).

### 3.3.3 Grain boundaries

In general, two grains meeting at a grain boundary are at an arbitrary crystallographic orientation to one another, and their easy magnetisation directions are not parallel (Goodenough, 1954). If the applied field is not sufficient to rotate the grain magnetisations out of their easy directions, there will be a discontinuity in the component of the magnetisation normal to the grain boundary, and free poles will be present. If the angles made by the magnetisations  $\mathbf{M}_S$  of the two grains with the normal to the grain boundary are  $\theta_1$  and  $\theta_2$ , the surface pole density at the grain boundary is:

$$\omega^* = \mu_0 M_S (\cos \theta_1 - \cos \theta_2) \quad (3.20)$$

Subsidiary domains may form at the boundary if the magnetostatic energy reduction achieved by this is larger than the domain wall energy required.

### 3.3.4 Models of domain wall dynamics

Two models of the ‘pinning’ of domain walls by microstructural defects have been proposed. The rigid-wall model considers an inflexible wall whose mo-

tion is retarded by statistical fluctuations in the density of defects, which modify the local potential energy. If defects are uniformly distributed on either side of the wall, the forces on it sum to zero, but otherwise a net force tends to move the wall to a more energetically favourable position.

The bowing-wall model, by contrast, allows the wall to bulge outwards between pinning points when a field is applied, before becoming detached when the wall area is too great. For some time, it was a subject of debate which of these models was correct (Hilzinger and Kronmüller, 1976).

### Potential energy model

Kittel and Galt (1956) proposed that rigid-wall motion could be modelled by considering fluctuations of potential energy with position. This model has been widely used as a qualitative description of wall energetics and dynamics (*e.g.* Craik and Tebble, 1965; Astié *et al.*, 1982; Pardavi-Horvath, 1999). Defects, such as inclusions and dislocations, locally modify the ‘constants’ characterising the exchange interaction and magnetocrystalline anisotropy. The resulting potential energy wells act as pinning sites, holding the walls in place until sufficient energy is supplied to free them.

Using such a model, it is possible to estimate the magnetic properties of a material by making assumptions about its defect distribution (*e.g.* Jiles, 1998). Also, since the derivative of potential energy with respect to distance,  $\partial E/\partial x$ , is proportional to the magnetic field required to move the domain wall, the defect distribution can be related to the external applied field (Pardavi-Horvath, 1999; Figure 3.5). However, because of the demagnetising effect, the applied field necessary for unpinning is greater than the unpinning field value calculated from this model (Kawahara, personal communication). Also, the critical unpinning field depends on the magnetisation state of the surrounding domains as well as the properties of individual defects (Pardavi-Horvath, 1999).

A potential energy model should characterise the energy of the ‘system’, *i.e.* the wall and its surroundings, rather than the wall alone (Cullity, 1972). For example, the interaction between a domain wall and an inclusion involves reduction of the wall energy by decreasing its area, and reduction of the local

magnetostatic energy by free pole redistribution.

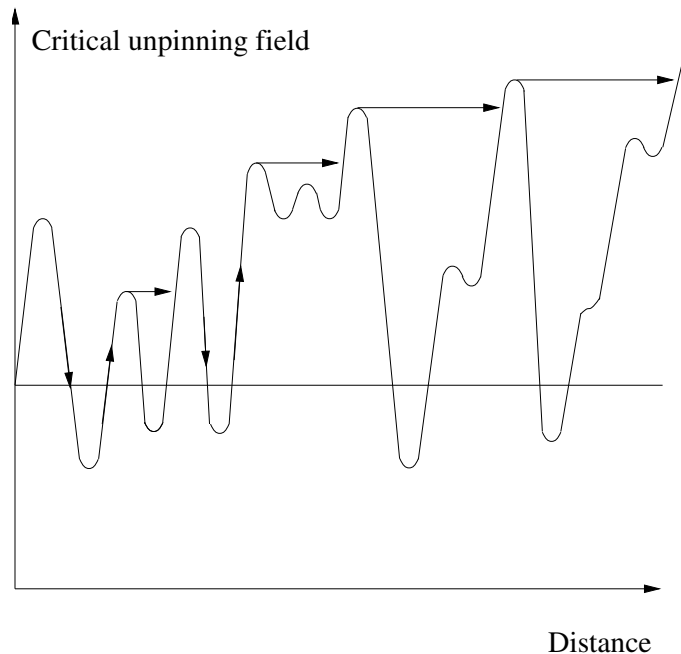


Figure 3.5: Field required for unpinning versus distance (adapted from Pardavi-Horvath, 1999). Arrows show the progress of a domain wall as the applied field increases. Once the field reaches a certain value, walls with critical unpinning fields less than this will not impede wall motion.

Certain microstructural features may act as potential energy maxima rather than wells (Pardavi-Horvath, 1999; Kawahara, personal communication). In this case, domain walls would be stopped, but not pinned, by the obstacle, and may lie close to, instead of directly on it. Some evidence of such behaviour has been observed by electron microscopy (Kawahara *et al.*, 2002).

### Models including bowing

Hilzinger and Kronmüller (1976) extended existing theories of rigid wall motion in statistical defect distributions (Träuble, 1966; Pfeffer, 1967) by allowing wall bowing. Curvature may occur parallel or perpendicular to the magnetisation direction, but in the perpendicular case, stray fields will result

since the wall is no longer parallel to an easy direction.

A computer simulation, using randomly distributed defects and wall-defect interaction forces of varying magnitudes, demonstrated that wall-bowing would occur given sufficiently large interaction forces (Hilzinger and Kronmüller, 1976). The two cases of rigid and bowing walls could be described by a single theory with a limiting condition separating the two types of behaviour. Curvature perpendicular to the magnetisation direction was also predicted when the wall-defect interaction energy was sufficiently high (Hilzinger and Kronmüller, 1977). When bowing occurs, the wall position is no longer determined simply by potential energy fluctuations; it was suggested that motion could instead be modelled using a frictional force.

### 3.3.5 Correlated domain wall motion and avalanche effects

Porteseil and Vergne (1979) found that experimental results for the magnetisation curve in a Fe-Si single crystal (composition not specified) could be reproduced using a model of ‘coupled’ domain wall motion, *i.e.* that the movement of one domain wall could stimulate another to move. The coupling was attributed to the modification of the distribution of free poles when the first wall moved. Tiitto (1978) also discussed the same possibility from the point of view of steel microstructure. He considered two possible methods for coupling between domain wall motion events. Firstly, there is direct magnetostatic coupling between domain walls at either end of a domain, and secondly, changes in the effective magnetising field occur as a result of magnetisation changes nearby. The first of these mechanisms was considered to be the stronger, because it would occur over a shorter range. Tiitto proposed a model of magnetisation based on such correlated motion, and proposed a relationship between grain size and magnetic Barkhausen noise (one of the macroscopic magnetic properties), based on this.

### 3.3.6 Mechanism of magnetisation reversal

Goodenough (1954) assessed the possible mechanisms of reverse domain nucleation. Inclusions and grain boundaries, at which subsidiary domain structures are known to occur in non-saturated samples, were proposed as nucleation sites. If the spike domains on large spheroidal inclusions are to contribute to magnetisation reversal, their magnetisation must be rotated against the anisotropy energy to become antiparallel to the bulk magnetisation. Goodenough showed that, in materials with cubic symmetry, the applied field required to accomplish this is too large for it to be a viable reversal mechanism. Even in uniaxial materials, in which the energy of reverse domain formation is lower, a very large field is required to detach the domains so formed from their nucleating particles. Goodenough therefore considered that spike structures of this kind did not contribute to magnetisation reversal.

At grain boundaries or planar inclusions, by contrast, Goodenough calculated the reverse domain formation energy to be much lower. Reverse domains were modelled as prolate ellipsoids and assumed to be continuous across the grain boundary. Figure 3.6 is a schematic of such a layout, based on the description by Goodenough.

A further site for domain nucleation suggested by Goodenough is the material surface. Unless parallel to an easy direction, this has free poles, which may be compensated by domain formation.

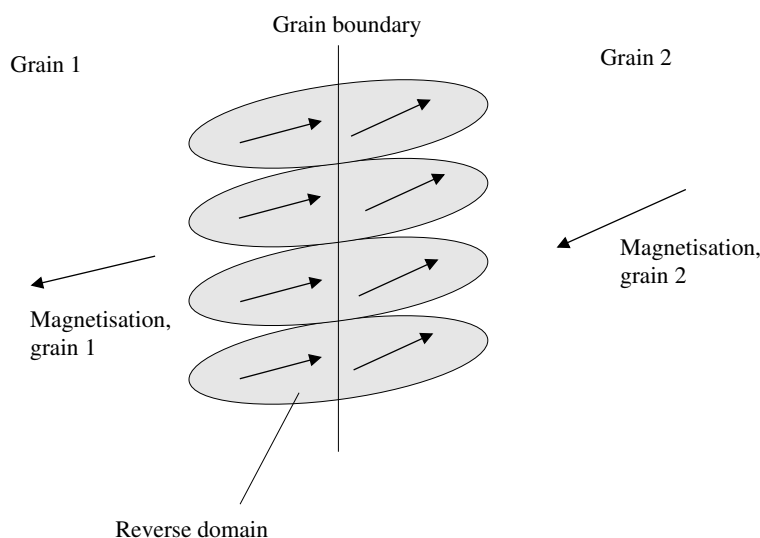


Figure 3.6: Reverse domain creation at a grain boundary (based on Goode-nough, 1954).

### 3.4 Direct observation of domains and domain walls

Many of the predictions of domain theory have been confirmed by direct observations of domains and walls using magnetic contrast techniques. The earliest images were obtained using a very finely divided magnetic powder suspended in a liquid and spread over the sample surface (Bitter, 1931). At positions where domain walls intersect the surface, the resulting stray fields attract the particles more strongly than do the surrounding regions (Kittel, 1949).

#### Magneto-optical effects

In optical microscopy observations, the interaction between magnetic fields and polarised light is used to obtain contrast. The plane of polarisation of an incident beam is rotated if it is transmitted through, or reflected from, a magnetised material (Williams *et al.*, 1951; Fowler and Fryer, 1952; Fowler and Fryer, 1956). These phenomena are known as the Faraday and Kerr effects respectively. The rotation angle depends on the component of the

magnetisation in the direction of the incident beam, which depends in turn on the magnetisation direction of the domain on which the beam impinges. Domain contrast is obtained by setting an analyser in the extinction position for one of the sets of domains. The Faraday effect is of limited use for domain imaging since it requires an optically transparent medium, but Kerr microscopy is used extensively.

### Electron microscopy

An electron beam incident on a magnetic domain is deflected in a direction determined by the domain magnetisation direction. In a transmission electron microscope (TEM), this can be used for magnetic contrast imaging ('Lorentz microscopy'). The beam deflection is extremely small, so no contrast is obtained using bright-field conditions, but by displacing the objective aperture so that only electrons deflected by certain sets of domains are allowed through, an image can be obtained in which some domains appear bright and others dark (Boersch and Raith, 1959). This is known as the Foucault method. Another technique, the Fresnel method, is used to observe domain walls. By going from an underfocused to an overfocused condition, domain walls change from bright to dark or *vice versa*. This enables domain walls to be distinguished from other features, such as dislocations, which do not show this behaviour (Hale *et al.*, 1959).

Scanning electron microscopy (SEM) techniques have also been developed. In highly anisotropic materials, in which the magnetisation has a component perpendicular to the surface, secondary electrons arising from a beam normally incident to the surface will be deflected in opposite directions by antiparallel domains. This gives rise to alternating light and dark bands in the secondary electron image (Type I contrast, Banbury and Nixon, 1969).

A method suitable for less anisotropic materials relies on the deflection of electrons after they enter the specimen (Type II contrast, Fathers *et al.*, 1973). The domain magnetisation direction governs whether deflection occurs towards or away from the surface, and hence determines the number of backscattered electrons emitted from that domain. This method requires a tilted specimen and a precise combination of electron beam parameters,

and has only successfully been applied in strongly magnetic materials such as Fe-3 wt. %Si (Jakubovics, 1994).

### 3.4.1 Surface domain structures

Subsidiary domain structures at sample surfaces, as predicted by Goode-nough (1954) have been observed in practice. Figure 3.7 illustrates the dependence of domain structures on the orientation of the surface plane in Fe-3 wt. % Si with no preferred texture (Nogiwa, 2000). Simple, banded domain structures were found when the plane normal was close to  $\{101\}$ . Near  $\{001\}$ , arrowhead-shaped domains formed in addition to the bands. Between  $\{101\}$  and  $\{001\}$ , the domain walls were wavy, and small, pointed domains occurred within larger domains of the opposite type. When the surface plane was close to  $\{111\}$ , the domain structure was fine and complex, and individual domains were difficult to resolve.

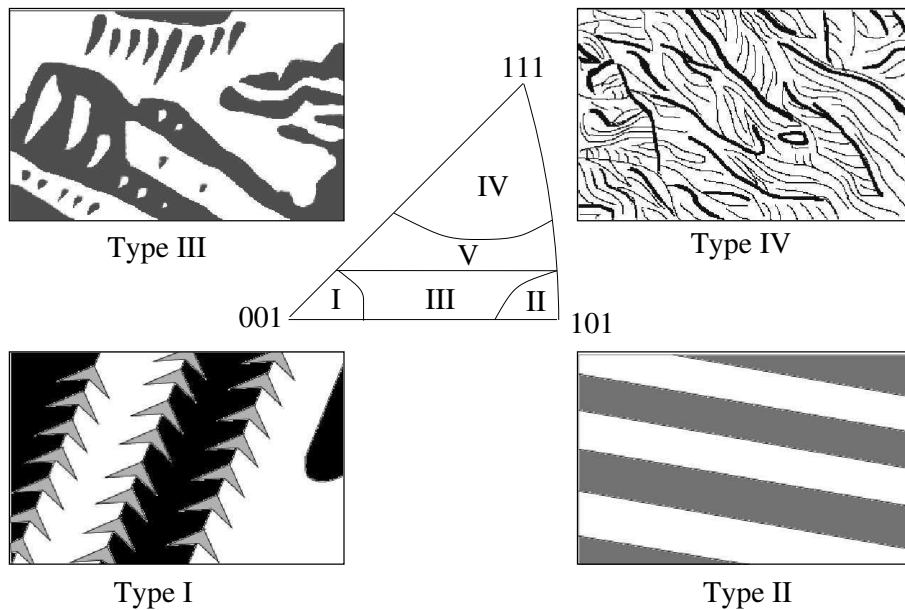


Figure 3.7: Effect of surface plane orientation on the domain structures observed in Fe-3 wt. % Si (Nogiwa, 2000)

The easy directions in Fe-3 wt. % Si are  $\langle 100 \rangle$ . In order for at least one easy direction to lie in a plane, by the Weiss Zone Law, one of the indices

$\{hkl\}$  of the plane must be zero, and for two perpendicular easy directions to be present, two of the indices must be zero. Hence, for  $\{101\}$  planes, only one pair of antiparallel easy directions lies in the plane, giving straight-sided domains (II). In  $\{100\}$  planes, the formation of domains magnetised at  $90^\circ$  to the main domains may occur (I). The  $\{111\}$  planes contain no easy directions so, in order to reduce the magnetostatic energy, a complex closure structure is generated on the surface (IV). The intermediate domain structure (III) occurs between  $\{001\}$  and  $\{101\}$ , so it should contain one easy direction.  $90^\circ$  walls are not allowed in this structure, so magnetostatic energy reduction occurs by the formation of small antiparallel domains within the main domains.

### 3.4.2 Magnetisation process in a single crystal

Figure 3.8 shows the evolution of the domain structure in annealed, single-crystal Fe-3.5 wt. % Si on increasing the applied field (Seeger *et al.*, 1969). The surface observed was parallel to the (100) plane, so that traces of  $180^\circ$  walls were parallel to  $\langle 100 \rangle$  directions, and traces of  $90^\circ$  walls were at  $45^\circ$  to  $\langle 100 \rangle$ . At low fields, magnetisation change occurred solely by the movement of  $180^\circ$  walls, and only when this could no longer occur did other walls begin to move. The  $90^\circ$  walls bounding thin spikes in (b) become fully developed echelon domain structures at higher field (c).

### 3.4.3 Domain wall behaviour at grain boundaries

The domain structures at grain boundaries in thin iron foils were observed by Lorentz microscopy (Tobin and Paul, 1969). The crystallographic orientations of the grains were determined using electron diffraction. Five distinct types of structures were identified. In the no-interaction case, the wall passes straight through the boundary (a). The ‘double spike’ domain structure is continuous across the grain boundary and magnetised antiparallel to the bulk (b). The ‘single spike’ domain (c), by contrast, stops at the grain boundary, and its magnetisation direction is at  $90^\circ$  to that of the bulk. The echelon structure (d) is a series of domains at  $90^\circ$  to one another, separated

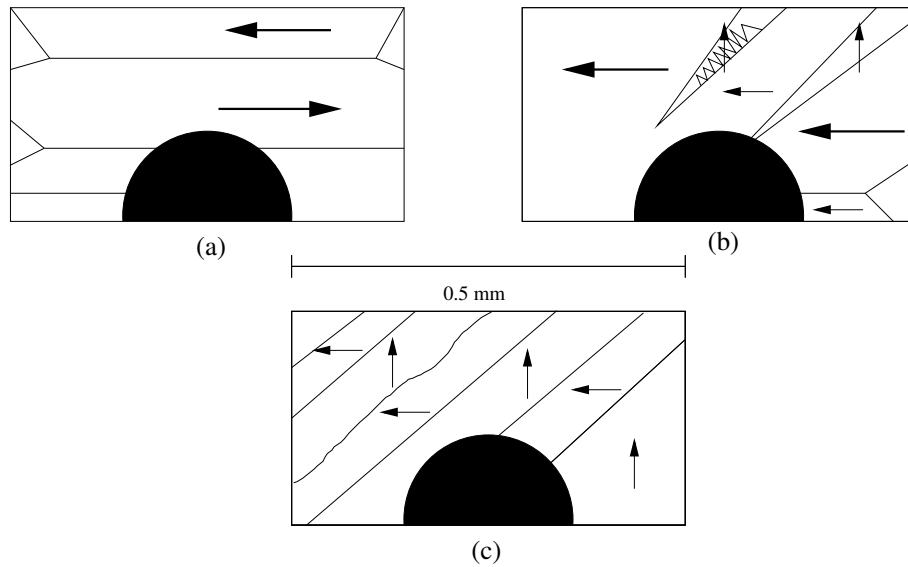


Figure 3.8: Domain structures in Fe-3.5 wt. % Si, observed by Bitter technique (Seeger *et al.*, 1969). (a) zero field; (b), (c) field increasing. The large black area is a dark area appearing on the original micrographs, perhaps due to surface damage.

from the bulk by a combination of  $90^\circ$  and  $180^\circ$  walls. The final case is the closure domain, in which the magnetisation direction is tangential to the grain boundary (e). Later observations by Degauque and Astié (1982) confirmed the existence of echelon domains and single spikes in annealed high-purity iron using high-voltage TEM on thicker foils.

The free pole density at grain boundaries can be estimated using Equation 3.20 if the magnetisation directions of the domains are known. Tobin and Paul estimated these, assuming that domains were magnetised approximately in the easy directions of iron and that the domain arrangement was consistent with minimising anisotropy and magnetostatic energy. By further assuming that magnetisation vectors lay in the plane of the foil, the pole density was calculated. This last assumption is valid if the anisotropy energy required for the magnetisation to lie in a non-easy direction along the surface is less than the magnetostatic energy for  $\mathbf{M}$  to have a component normal to the surface.

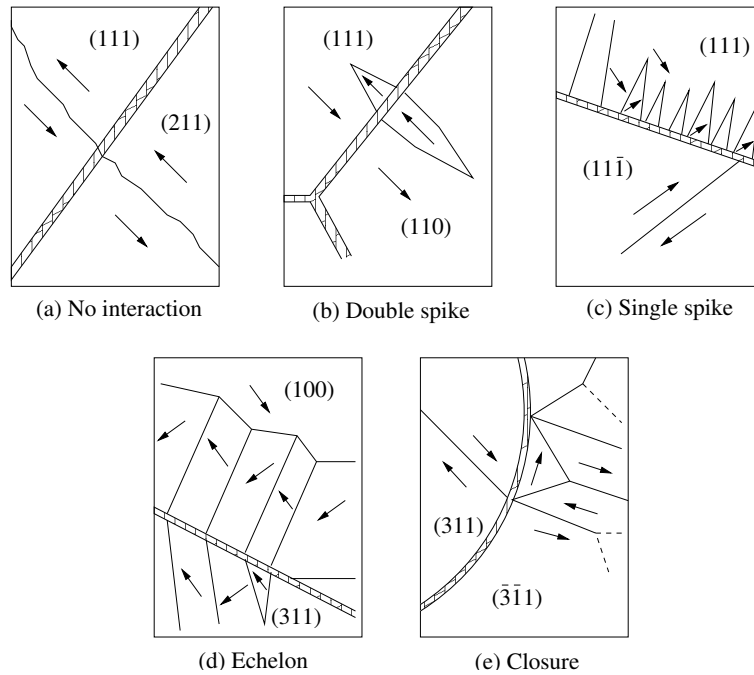


Figure 3.9: The five types of interaction between grain boundaries and domain walls, shown in order of increasing magnetic pole density at the grain boundary (Tobin and Paul, 1969).

The no-interaction and double-spike configurations were found to have the lowest pole densities, and closure domains the highest, with single-spike and echelon structures in the low-to-intermediate range. It is notable that  $90^\circ$  walls do not occur at low pole densities.

The observations of double spike domains are consistent with the theoretical analysis of Goodenough (1954), but he did not predict the existence of  $90^\circ$  closure walls at grain boundaries. It appears that if an easy direction occurs parallel to the wall, it is favourable to form such a closure domain. These domains, unlike the  $180^\circ$  reverse spike domains, are not expected to contribute to magnetisation reversal according to the arguments of Goodenough.

Lorentz microscopy observations of domain walls and grain boundaries during the magnetisation of spinel ferrites showed that if a domain wall was parallel to a grain boundary, the wall was stopped completely by the

boundary (Lin *et al.*, 1984)<sup>3</sup>. If the wall intercepted the grain boundary obliquely, its progress was retarded, with the least retardation occurring when the boundary and wall were normal to one another.

Closure domains were observed at grain boundaries in ferritic steel using Lorentz microscopy (Hetherington *et al.*, 1987). Domain walls were attached to triple junctions, and grains contained a substructure of domains which needed only a small applied field to move.

### 3.4.4 Effect of grain boundary misorientations

At a grain boundary, two differently oriented crystal lattices meet. One of the ways to characterise the geometry of grain boundaries is the coincidence site lattice (CSL) concept, which is discussed in more detail in Chapter 7. If the lattices from the two grains are superposed, with a common origin, then for certain pairs of grain orientations, a fraction of the lattice points of the two grains will coincide. The superlattice of coincident lattice points is a CSL, and is characterised by a parameter  $\Sigma$ , where  $1$  in  $\Sigma$  of the lattice points are coincidence sites. The  $\Sigma$  notation is applied to boundaries between grains whose lattices form, or nearly form, a CSL. Closer matching is expected at such boundaries than at those with no special orientational relationship, which are known as random boundaries. Low-angle boundaries are those in which the difference in orientation angle between the adjacent grains is  $\leq 15^\circ$ . This misorientation is accommodated by a periodic array of dislocations.

#### Low-angle and random boundaries

Figure 3.10 (a) and (b) show schematically the domain arrangements observed at a low-angle grain boundary in Fe-3 wt. % Si using Kerr microscopy (Kawahara *et al.*, 2000). At one position, the domains were almost continuous across the boundary (a). In another region, the structure was disrupted, but the domains formed on the boundary were relatively large (b).

---

<sup>3</sup>Spinel ferrites are ferrimagnetic but, because they have a similar domain structure to ferromagnetic materials, these observations are still useful for understanding ferromagnetic domain wall behaviour.

At a random boundary the structure was in one region discontinuous (Figure 3.10 (c)), and in another continuous, with inclination of the bands (d).

The free pole density at a grain boundary depends not only on the angle between the magnetisation vectors in the adjacent grains, but also on the local orientation of the grain boundary with respect to these vectors (Shilling and Houze, 1974). It is very much reduced if the boundary approximately bisects the angle between the magnetisation vectors. This accounts for the difference between the domain structures in Figure 3.10 (c) and (d) (Kawahara *et al.*, 2000). In (c), the boundary is in an asymmetric position, resulting in a complex domain structure, but in (d), the symmetric arrangement allows simple banded domains to continue across the boundary.

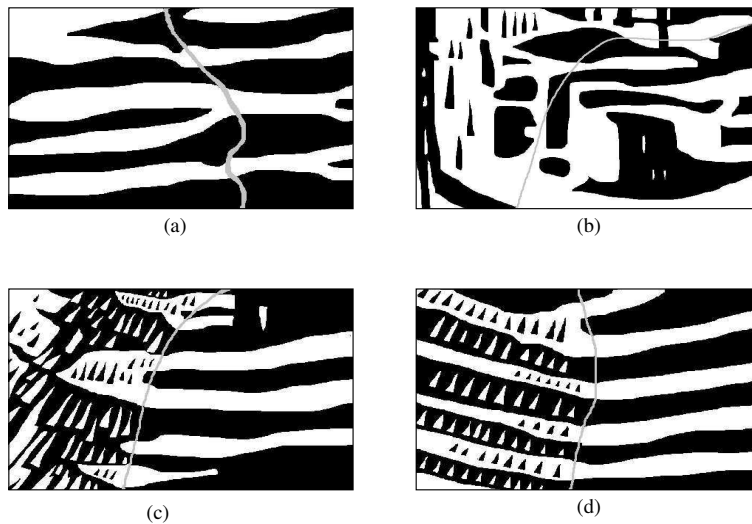


Figure 3.10: Domain structures observed at grain boundaries in Fe-3 wt. % Si by Kerr microscopy (schematic): (a), (b) low-angle boundary, (c), (d) random boundary (Kawahara *et al.*, 2000).

Significant differences were observed between low-angle and random boundary domain structures during magnetisation. At the low-angle boundary, only a small applied field was required to transform the arrangement in Figure 3.10 (b) into one of parallel-sided domains. As the field was increased, one set of domains gradually widened at the expense of the antiparallel set. The grain boundary appeared to act as a domain source, at which new do-

mains nucleated, and a sink into which they disappeared. At the random boundary, no abrupt changes were observed. Instead, one set of bands grew gradually at the expense of the other until the majority of the region was a single domain containing small antiparallel spikes.

Kawahara *et al.* discussed the possible influence of grain boundary stress fields, as well as free poles, on the domain structure. Because of the dislocation arrays at low-angle boundaries, the strain energy is expected to be higher than at random boundaries, where there is no periodic structure (Kawahara, personal communication). If magnetoelastic effects were the predominant source of domain wall-grain boundary interaction energy, this interaction would instead be stronger at low-angle boundaries, but since this is not so, it appears that magnetostatic energy from misorientation is more important.

### Coincidence boundaries

Lorentz microscopy was used to study the interactions between domain walls and grain boundaries of different types (Kawahara *et al.*, 2002). Domain walls were observed lying directly on grain boundaries, in a ceramic ferrite sample. A triple junction between low-angle grain boundaries acted as a pinning site, holding in place five domain walls. A void also acted as a domain wall attractor, bending walls towards itself.

In a sample of pure nickel, domain walls were initially only observed on one side of a random boundary. On changing the applied field, the walls moved gradually towards the boundary but, as they approached closely, the domain configuration changed abruptly, and reverse domains appeared in the neighbouring grain. The domain wall moved so that part of its length lay along the boundary, before breaking away in another abrupt change.

Figure 3.11 is a schematic of another observation on pure nickel in which a similar combination of gradual and sudden processes was seen. The interactions between domain walls and grain boundaries depended on the angle of approach. Walls almost normal to a grain boundary were affected very little by it (a), but those approaching at a small angle were deflected to lie parallel to the boundary (b). This confirms the findings of Lin *et al.* (1984). However, low-angle boundaries were an exception, interacting only weakly

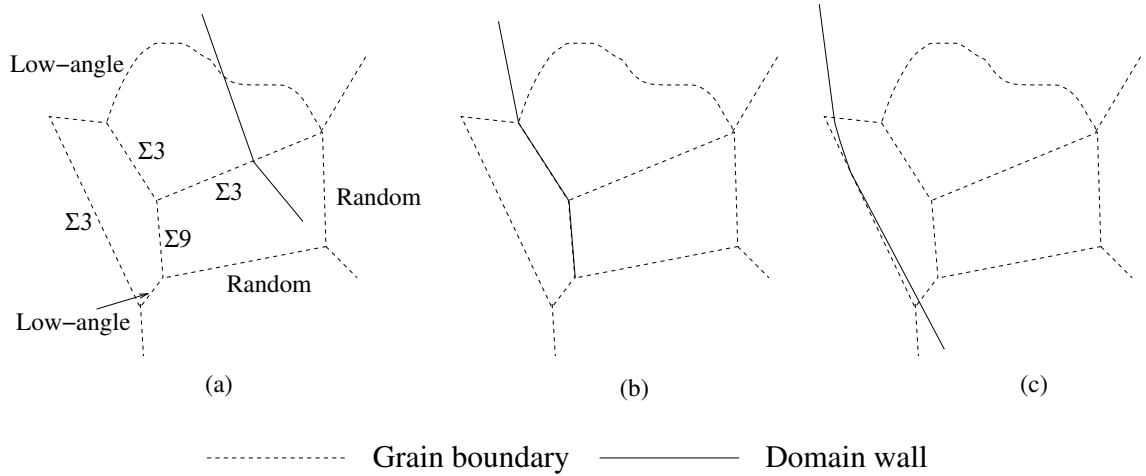


Figure 3.11: Interaction between a domain wall and grain boundaries of different types (schematic): (a) Domain wall interacts weakly with  $\Sigma 3$  boundary because of almost perpendicular approach. Weak interaction between wall and low-angle boundary despite small impingement angle. (b) Domain wall jumps to lie parallel to  $\Sigma 3$  boundary. (c) A jump to another  $\Sigma 3$  boundary, but the wall appears to lie beside the boundary rather than on it (Kawahara *et al.*, 2002).

with domain walls even when approached at a small angle (Kawahara *et al.*, 2002).

On close inspection, domain walls appeared to lie just beside  $\Sigma 3$  boundaries, but directly on random boundaries. Domain walls in potential energy wells would be found at the centre of the well, but walls impeded by potential energy maxima would be stopped some distance from the centre of the maximum. It was therefore suggested that random boundaries acted as wells, and  $\Sigma 3$  boundaries as maxima.

### 3.4.5 Effect of grain size

In nanocrystalline nickel, with grain size  $< 1 \mu\text{m}$ , domain walls lay along grain boundaries for almost the whole of their length, only rarely passing into the grain interior (Kawahara *et al.*, 2002). This contrasts with the behaviour seen in Figure 3.11, in which the grain size was several tens of

$\mu\text{m}$ . The greater concentration of grain boundaries in the nanocrystalline sample allows domain walls to lie on grain boundaries without significant deviation.

The domain width in Fe-3 wt. % Si increased with increasing grain size (Shilling and Houze, 1974). A grain boundary is more likely to be in an approximately symmetrical position between the magnetisation directions in adjacent grains when the misorientation angle between the grains is small. This becomes less likely with decreasing grain size. Larger demagnetising fields, and the consequent development of a finer domain structure, is therefore likely in finer-grained materials.

### 3.4.6 Effect of deformation

Heavy deformation of a Fe-3.5 wt. % Si single crystal produced a domain structure in which only one pair of antiparallel magnetisation directions was represented, even though directions perpendicular to these were permitted by symmetry (Seeger *et al.*, 1969). Deformation is believed to favour  $180^\circ$  over  $90^\circ$  wall motion because  $90^\circ$  walls interact more strongly with stress fields, becoming immobilised in a highly dislocated structure.

In-situ magnetising experiments on annealed, lightly deformed and heavily worked samples of pure iron demonstrated the pinning effect of dislocations on domain walls (Degauque and Astié, 1982a). The annealed material contained a few small tangles of dislocations, which acted as strong pinning sites, retarding the movement of the domain walls to which they were attached while other, unpinned domains moved more freely. Mixed dislocations in the lightly strained sample and long screw dislocations in the heavily worked sample also pinned domain walls. Work on macroscopic magnetic properties suggested that domain wall motion was more strongly pinned in the heavily worked sample (Astié *et al.*, 1981), but such differences were difficult to discern using TEM.

### 3.4.7 Second-phase particles and microstructural differences

#### Lath microstructures

Domain structures in bainitic and martensitic forms of the same carbon-manganese steel composition were compared (Beale *et al.*, 1992). In specimens with long, parallel laths, a regular structure of  $180^\circ$  walls, branching into  $90^\circ$  walls, was observed. In a sample in which only part of the structure contained laths, the domain walls were found to stretch across the laths, and to move parallel to them when the field was applied. Apart from this one study, domain arrangements in lath microstructures do not seem to have been studied extensively.

#### Ferritic-pearlitic steels

Hetherington *et al.* (1987) concluded that the domain wall arrangement in pearlitic steels depended on the orientation of the walls with respect to the cementite lamellae. If a wall lies parallel to a lamella, it is strongly pinned, whereas if it is perpendicular, it moves easily until it meets another grain in which the lamellae are oriented differently.

It is also believed that the lamellar spacing plays an important role in the domain layout (Lo *et al.*, 1997a). Small spacings gave small domains which were mainly bounded by Type-II walls following the ferrite/cementite interface. When the spacing was larger, domains extended across several lamellae, and Type-I walls were observed. Dynamic magnetisation experiments showed that in the finer pearlite, the nucleation and growth of reverse domains required a higher applied field, and individual domain wall jumps were smaller.

In both fully pearlitic and fully ferritic microstructures, domains of reverse magnetisation nucleated when the field was reduced from saturation, but the growth of domain walls across the grain occurred more rapidly in the ferritic sample (Lo and Scruby, 1999). In the pearlitic sample, it did not occur until the applied field direction had been reversed. These findings demonstrate the pinning strength of pearlite lamellae.

### Lamellar and spheroidal cementite

The pinning effect of lamellar and spheroidised pearlitic microstructures were compared (Lo *et al.*, 1997b). In both cases, the cementite particles acted as domain wall pinning sites, but coarser domains were observed when the carbides were spheroidal. On reduction of the field from saturation, domain wall motion required a larger reverse field in lamellar than in spheroidised pearlite. Closure domains were observed on the carbide particles in the spheroidal microstructure, and these interacted with the  $180^\circ$  walls as they moved.

The results from experiments on pearlite show that lamellar particles are a more effective impediment to domain wall motion than spheroidal particles. This may be due to the flat, continuous nature of the particles, or to their parallel, regularly spaced arrangement, or to a combination of both. It does not appear that any observations have been made on needle- or plate-shaped particles such as  $M_2X$  in tempered steels. If the flat, elongated shape is the more important factor in pinning, these particles, too, would act as strong pinning sites. However, if parallelism is more important, then  $M_2X$  may only pin weakly since it tends to be small.

## 3.5 Conclusions

Experimental observations of domain structures in ferromagnetic materials show a remarkable agreement with the theory which, in some cases, pre-dated them by several decades. It has been shown that domains interact with grain boundaries, inclusions and dislocations. Some of the main findings from these studies are as follows:

- Cubic or spheroidal inclusions interact with domain walls by wall area reduction and by setting up demagnetising fields. Inclusions larger than a critical size have subsidiary spike domains.
- Lamellar precipitates in steel have a stronger pinning effect on domain walls than do spheroidal precipitates.

- Specimen surfaces nucleate fine domains to reduce magnetostatic energy if they are not parallel to crystallographic planes containing easy directions.
- It has been observed that at low values of applied field, magnetisation change occurs preferentially by  $180^\circ$  wall motion.
- Domain walls tend to be attracted towards voids and grain boundary triple (or multiple) junctions.
- The domain structure at grain boundaries depends on the misorientation between the adjacent grains, and on the angle made by the grain boundary plane with the grain magnetisations.
- The dynamic interaction between grain boundaries and domain walls depends on the angle at which the domain wall intercepts the grain boundary, and also on the grain boundary character. Low-angle boundaries exert a weaker pinning effect than boundaries of other types.
- The width of domains has been observed to increase with increasing grain size.
- In a material with finer grains, domain walls were observed to lie along grain boundaries for far more of their length than in coarser-grained material.
- It is predicted that reverse domains should nucleate on grain boundaries, surfaces and planar inclusions, but not on cubic or spheroidal inclusions.